TELKOMNIKA, Vol.17, No.5, October 2019, pp.2235~2243
ISSN: 1693-6930, accredited First Grade by Kemenristekdikti, Decree No: 21/E/KPT/2018
DOI: 10.12928/TELKOMNIKA.v17i5.11930

Design of wideband Rotman lens for wireless applications

Mohammed K. Al-Obaidi*[1], Ezri Mohd[2], Noorsaliza Abdullah[3], Samsul Haimi Dahlan[4]
[1,2,3,4]Department of Communication Engineering, Faculty of Electrical and Electronic Engineering, Universiti Tun Hussein Onn Malaysia (UTHM), Johor, Malaysia
[1]Department of Network Engineering, Faculty of Engineering, Al-Iraqia University, Baghdad, Iraq
*Corresponding author, e-mail: al.obaidi.m.k.i@gmail.com

Abstract

An electrically steerable beam is an essential standard in the recent wireless application in order to increase the gain and reduce the interference. However, high performance of amplitude besides low phase error difficult to achieve without indicators are used to set lens parameters to desired optimum performance design level. In this paper, the introduced microstrip lens has examined a comprehensive explanation for parameters and indications amid a full wave structure methodology. Further, Phase and energy coupling between excited ports and received ports besides phase error and its relation with the lens parameters design are explained in detailed. A wideband beamforming network based on a printed microstrip Rotman lens with a ±26º scanning angle was designed in this study. The designed lens operates at 2.45 GHz with 592 MHz bandwidth. The lens consists of five switchable ports (input ports) with four output ports that connected to the microstrip patch antennas. The five switchable ports were used to realize the scanning beams angle in the azimuth plane. The proposed model is simulated by CST Microwave Studio and fabricated on FR-4 with 1.565 mm thickness and 4.2 permittivity. A good agreement between simulation and measurement results were achieved.

Keywords*: beamforming ISM band, Rotman lens, steerable antenna*

1. Introduction

A wireless communications system in recent years is directed to become smarter in order to achieve high data capacity and better quality. A beamforming technique considered a key technology for this rapid development in smart antenna system applications [1-5]. Butler matrix, Blass matrix, and its modified design Nolen matrix are the earlier generation types of beam forming network BFNs. Nevertheless, the complexity of the pattern and the dependency of the shifting beam on the frequency are the most drawbacks of these techniques besides its narrow bandwidth in microstrip model [6-9].

The Conventional Rotman lens is a true time delay (TTD) BFNs which depends on the path delay in order to achieve the desired phase shift [10]. Low profile, compactness, low phase error and easy to fabricate as microstrip model are the most advantages of the Rotman lens. Many civilian and military applications are based on the Rotman lens to control the radiation beam scan angle such as automotive platform sensing [11], radar applications [12] and satellite communication [13].

There are three main field of study discussed Rotman lens performance analysis. First field is focused on the parameters design development in order to provide more freedoms in the model design besides taking the phase error in the consideration [14-18]. While the second scope interested on the approaches to determine phase and amplitude of the beams at the aperture [19, 20]. Finally, third field of Rotman lens is discussed a methods used to design a complete algorithm to build and optimize a complete lens structure using computer aided design [21, 22].

Lens performance determination has a level of complexity in order to achieve the desired goal of phase and amplitude stability along frequency bandwidth. Therefore, this work has two objectives, first objective is to explain a full wave lens design procedures step by step by applying comprehensive parametric study in terms of phase error level for lens structure including beam countor, receive countor, on-focal length, off-focal length and the eccentricity of

Received November 29, 2018; Revised April 17, 2019; Accepted May 19, 2019

beam countor. While the second objective is proposed an implementation of microstrip Rotman lens to scan the azimuth plane with coverage angle ±26º and the operating frequency of the design is selected to be in Industrial, Scientific, and Medical (ISM) radio band.

In general, the structure of the lens is a multiport device with three types of ports as shown in Figure 1. Firstly, the beam ports are the input ports to the lens cavity which is the desired frequency will be applied. Secondly, the receive ports that receive the energy from the beam ports to deliver it to the connected array elements of the transmission line. Finally, he side wall of the cavity lens will be terminated by the dummy ports and 50Ω loads to absorb energy and reduce the reflections inside the lens cavity which are affected directly thephase performance.

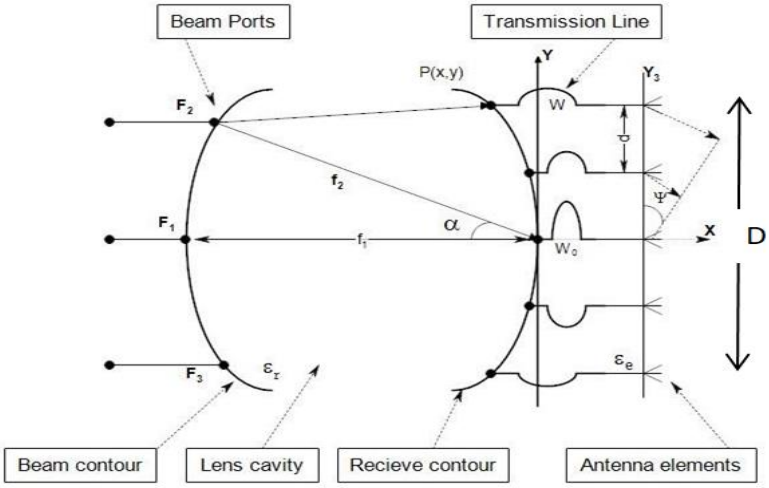

Figure 1. Rotman lens geometry [10]

2. Research Method

This section of the study will be divided into three subsections. In the first section, Rotman lens design equation and parameter definition will be explored. While in the second section, parametric study for lens design procedure beside its relation to the phase error will be discussed in details. Finally, the proposed lens design at 2.45 GHz and a final lens CST model will be implemented and explained.

2.1. Rotman Lens Parameters and Design Equations

Beamforming techniques in a linear phased array system are depending mainly on the linear phase shift which feeds the radiated elements in ordered to form the radiation pattern in the desired angle [6]. The standard excitation system provides only one excitation port with specific magnitude and phase. In order to produce a multi-phase shift a BFNs is applied. The Microstrip Rotman lens model is a structure can provide a progressive phase shift to the radiation pattern, the position of the three focal points (F_1, F_2, and F_3) on the beam contour has theoretically free phase error with a unique subtended angle (α). These focal points are placed in the beam contour.

The shape of the beam contour can be circular or elliptical depends on the lens shape and the phase error level. While receiving ports placed on the receive contour at (X, Y) coordinate. Array elements connected to receive contour by transmission lines with length (W). The length of transmission lines saves the phase reach each array element. The distance between adjacent array elements is (d). The beam width of the radiation pattern and the sidelobe level can be controlled by adjusting (d) value [23]. However, in this study, the lens modeled using microstrip transmission line theory, but it can be designed using different materials permittivity (ε_r) and (ε_e). The subtended angle (α) can be the difference from a radiation beam angle (Ψ) in order to give more freedom design ability [14, 15, 24]. The final lens structure will have low impedance due to its large area compared with the 50Ω transmission

line. In order to balance the impedance between the lens cavity and a transmission line, a transformation impedance must be used. In the general tapering line between the transmission line and the lens cavity will be used to decrease the discontinuity and match the impedance of the lens cavity with 50Ω. An optimization process will be carried out to the length of taper to determine the best return loss of the ports in the range of operating frequency. However, a quarter wavelength multi-sections lines can be used to match between the lens cavity and transmission line. The length sections can be determined using a standing wave pattern [25]. By equalizing the path from the three focal points to the phase front of the lens the design equations can be derived as follows [26]:

$$w = \frac{\sqrt{\varepsilon_e}}{\sqrt{\varepsilon_r}} \frac{-b \pm \sqrt{b^2 - 4a\,c}}{2a} \tag{1}$$

$$x = \frac{Y_3^2 \sin^2 \psi}{2\varepsilon_r (\beta \cos\alpha - 1)} + \frac{(1-\beta)\, w}{\beta \cos\alpha - 1} \sqrt{\frac{\varepsilon_e}{\varepsilon_r}} \tag{2}$$

$$y = \frac{Y_3 \sin\psi}{\sqrt{\varepsilon_r}\, f_1 \sin\alpha} \left(1 - \frac{w}{\beta} \frac{\sqrt{\varepsilon_e}}{\sqrt{\varepsilon_r}}\right) \tag{3}$$

$$\text{Where:} \quad a = 1 - \left(\frac{1-\beta}{1-\beta C}\right)^2 - \frac{\zeta^2}{\beta^2 \varepsilon_r}, \; b = -2 + \frac{2\zeta^2}{\beta \varepsilon_r} + \frac{2(1-\beta)}{1-\beta C} - \frac{\zeta^2 S^2 (1-\beta)}{(1-\beta C)^2 \varepsilon_r}$$

$$c = \left(-\zeta^2 + \frac{\zeta^2 S^2}{1-\beta C} - \frac{\zeta^2 S^2}{1-\beta C} - \frac{\zeta^2 S^4}{4(1-\beta C)}\right) \frac{1}{\varepsilon_r}$$

$$\beta = \frac{f_2}{f_1}, \; \zeta = \frac{Y_3 \sin\psi}{f_1 \sin\alpha}, \; S = \sin\alpha, \; C = \cos\alpha$$

where the values: *x, y*, and *w* are normalized to on-focal length axis f_1.

2.2. Parametric Study for Lens Geometry

Rotman lens is a structure used to achieve a linear phase shift to radiation elements in order to form different beams to scan specific angles. So, the design parameters related directly to the phase error. In this section, a parametric study to the lens design parameters will be conducted besides its relation to the phase will be explained. The relation between the off-focal physical length (f_2) and on-focal physical length (f_1) is the parameter (β) which consider the main optimization factor of the phase error. It is realized from a parametric investigation that the beam contour becomes flatter and the receiver contour shrinks when the value of (β) increased as Figure 2 described.

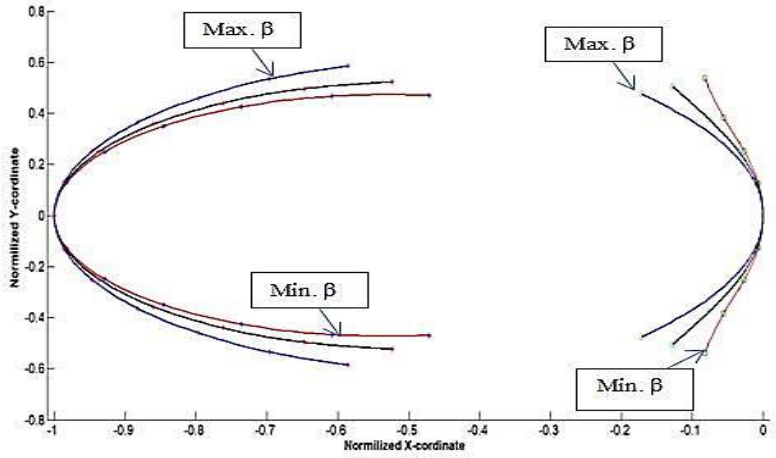

Figure 2. Lens contour shape versus β

The tri-focal Rotman lens contains three focal points with zero phase error, however, to achieve more than three scan steps a nonfocal point must be introduced. These non-focal points have a phase error, on other terms, non-focal points do not apply the path length equalities which is considered the first step to drive lens design equations [27]. The phase error of multi (β) is examined as Figure 3 described. The area under the curve indicates that the maximum phase error at β=0.85.

According to the parametric study, the beam contour circular shape has a small difference phase error value compared with the elliptical one as Figure 4 described, which (e=0) is referred to circular beam contour. However, the elliptical shape can be used in the large model to point the beam taper direction to receiver ports and reduce phase error [24].

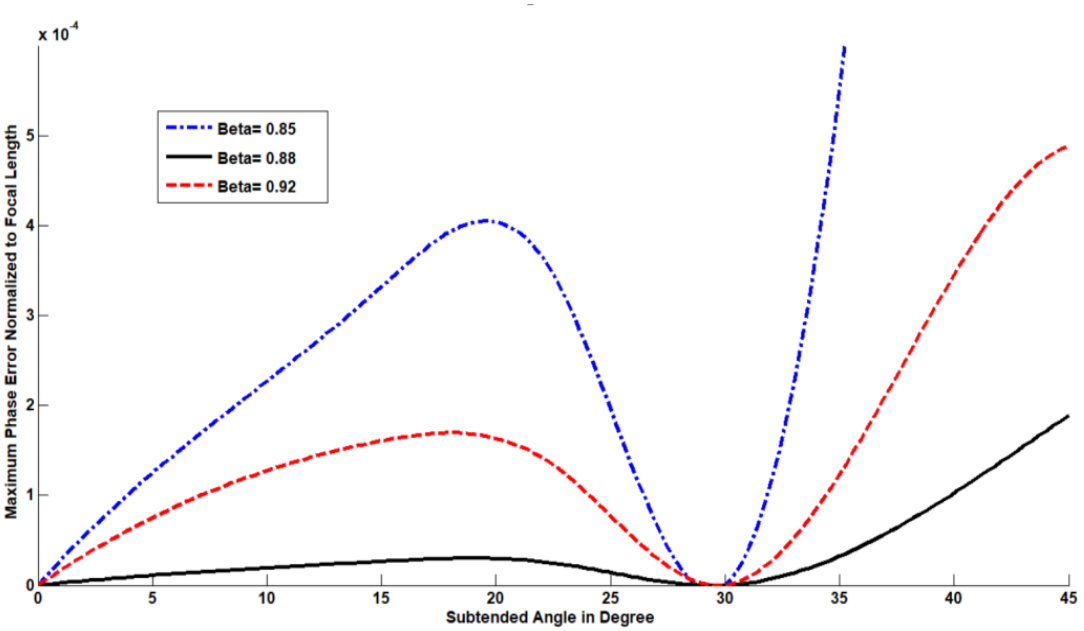

Figure 3. Maximum phase error versus beta parameter

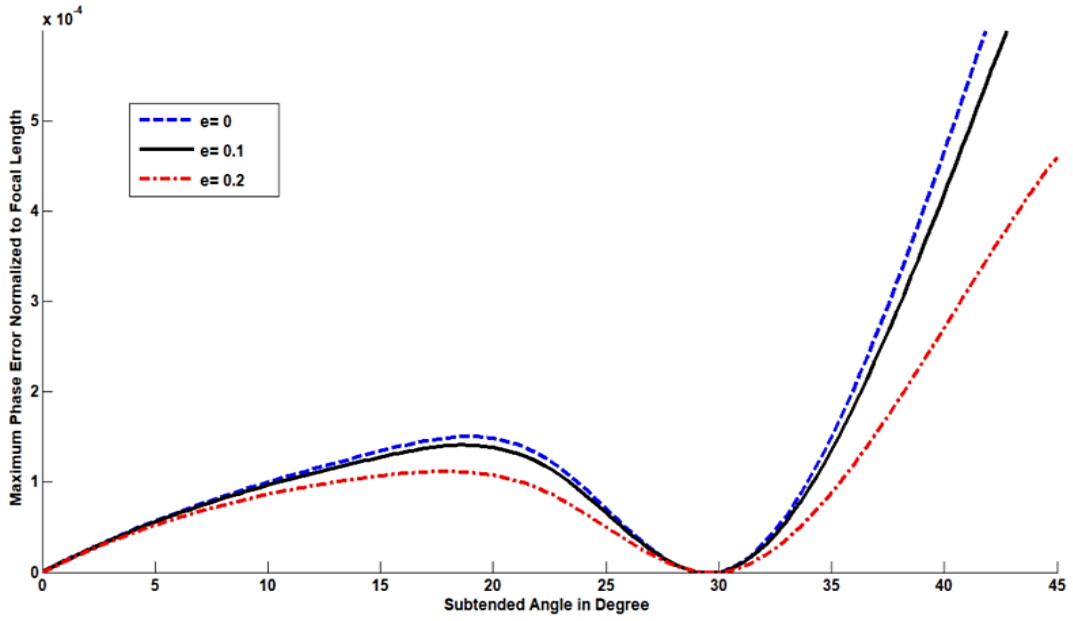

Figure 4. The eccentricity of beam contour versus phase error

Finally, the relation between aperture length (D) and focal length (f_1) is considered an important factor in the phase error optimization as Figure 5 explained. It can be noted that the length of (D) related to aperture size of the lens and the value of (f_1) is a normalized factor effect to the overall dimensions of the lens besides the bandwidth of operating frequency.

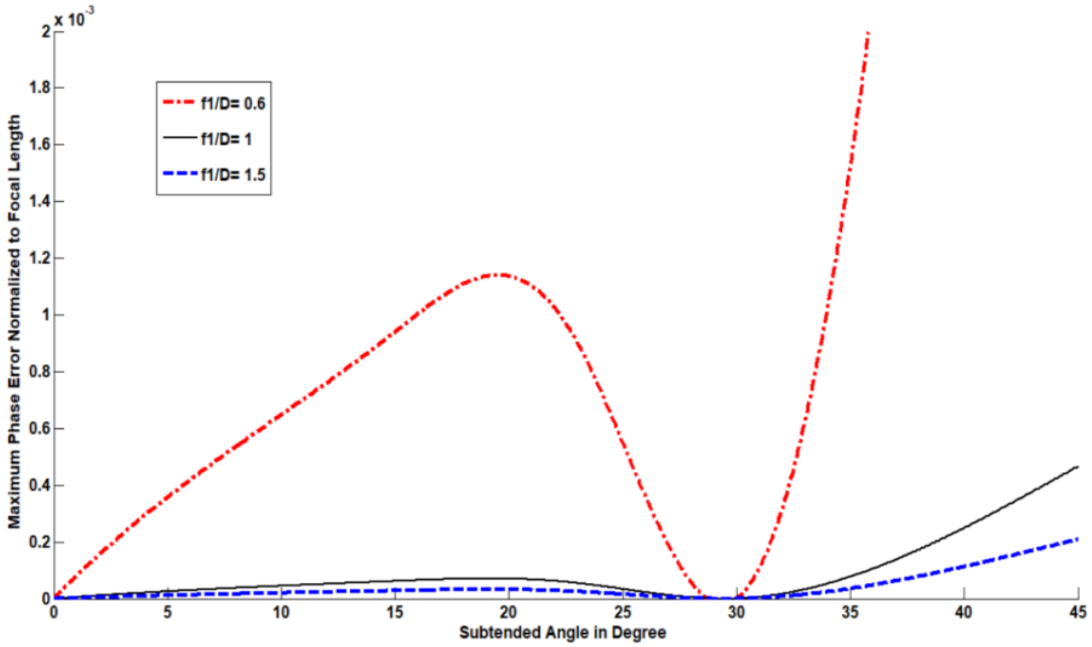

Figure 5. f_1/D versus phase error

2.3. Simulation and Measurements Results

In this section, Microstrip Rotman lens will be constructed using the design parameters explained in Table 1. The lens geometry is determined using MATLAB and the model is simulated using CST Microwave Studio. The calculated beam lens and receiver contour besides the port locations are explained in Figure 6.

Table 1. Lens design specifications

Design variable	Value	Design variable	Value
No. Of beam ports	5	Focal length (f_1)	1.45 λ_g
No. Of antenna ports	4	Displacement, distance (d)	0.43 λ
No. Of dummy ports	8	Substrate thickness	1.565 mm
Scan angle (α)	±26°	Length	209.52 mm
Relative permittivity (ε_r)	4.2	Width	203.62 mm
Loss tangent	0.025	Center frequency	2.45 GHz
Copper thickness	0.035 mm		

Tapering ports will be used in the final lens model in order to guarantee a smooth energy transition from input ports to the lens cavity and receiver ports to radiated elements. The optimization process is conducted to achieve an acceptable return loss for tapering ports [28]. Eight tapered dummy ports with 50 Ω load will terminate the side wall in order to reduce the reflections inside the lens cavity and the phase performance. The full lens structure with five beam port order (1-5), four receivers (6-7) and eight dummy ports (10-17) is shown in Figure 7. It can be concluded from the lens geometry that the number of beam ports is related to the scan steps and the number of the receiver ports is proportional with radiated elements, on other words, when the number of radiated elements is increased a high gain radiation beam will be achieved.

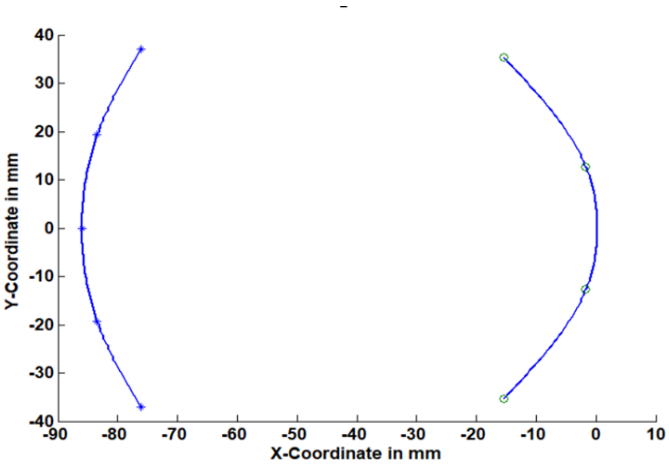

Figure 6. Lens geometry

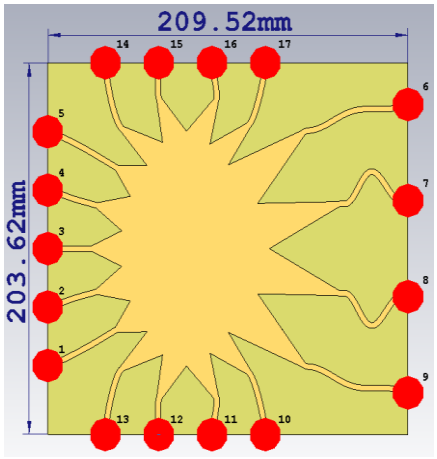

Figure 7. Lens structure CST model

3. Results and Analysis

In this section, the fabrication process for the CST lens model is conducted. While the simulation results for the beam ports return loss and the coupling including phase and energy between beam ports and receive ports obtained by Microwave CST Studio are validated by measurements. Finally, the radiation pattern using array elements will be tested.

The lens performance is related to the return loss and phase performance. The full matrix s-parameters are tested using CST Microwave Studio and validated by vector network analyzer measurements. The return loss of beams ports is shown in Figure 8. An acceptable return loss below -10 dB in the bandwidth range (2.1811-2.774 GHz) is achieved for beam ports. It can be noted that only three beam ports are shown in Figure 8 due to symmetrical geometry. In addition as a comparable to the lens reported in [29], it can be realized the effect of the lens dimension specially the on-focal length to the bandwidth range as a results of minimizing the focal length the bandwidth became narrower.

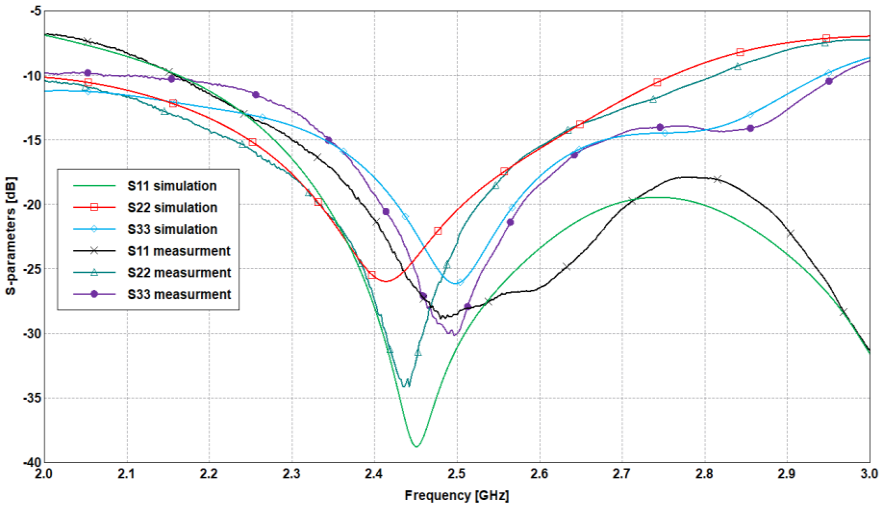

Figure 8. Beam ports return loss

The linear phase shift is the main objective in the lens to direct the beam into angles. The linearity in the phase shift when beam ports are excited by 2.45 GHz is shown in Figure 9. It can be noted that the phase shift for the port3 across the receive ports close to being zero in order to form the radiation beam at a zero scan angle as will be explained in the next section. Otherwise, the phase shift for the port two and three is increased across the receive ports.

Coupling between beam ports and receive ports are an indication about the energy reached to the radiation elements from the excitation ports. The results indicated that an even energy is distributed across receive ports when beam ports is excited at 2.45 GHz with a maximum fluctuation about 3 dB as shown in Figure 10.

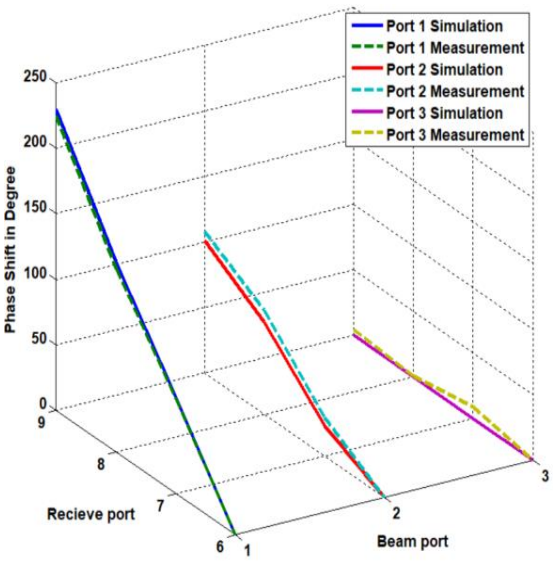

Figure 9. Phase shift for beam ports at 2.45 GHz

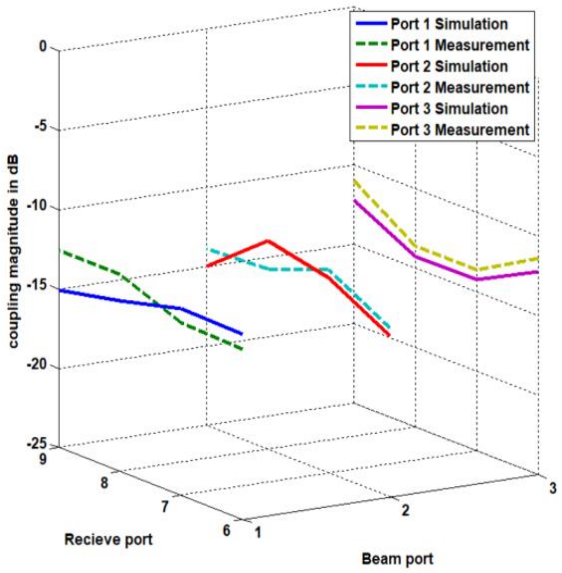

Figure 10. Coupling magnitude across receive ports at 2.45GHz

In order to test the radiation pattern of the lens four microstrip patch antenna with center frequency at 2.45 GHz are designed and fabricated to connect it to the lens by the right angle SMA connector. The full beamforming system is described in Figure 11. After measurements of the scattering parameters of the fabricated lens, the radiation pattern measurements will be carried out in order to realize the beams and the scanning angle switching. The measurement is conducted in the anechoic chamber and the setup is shown in Figure 12.

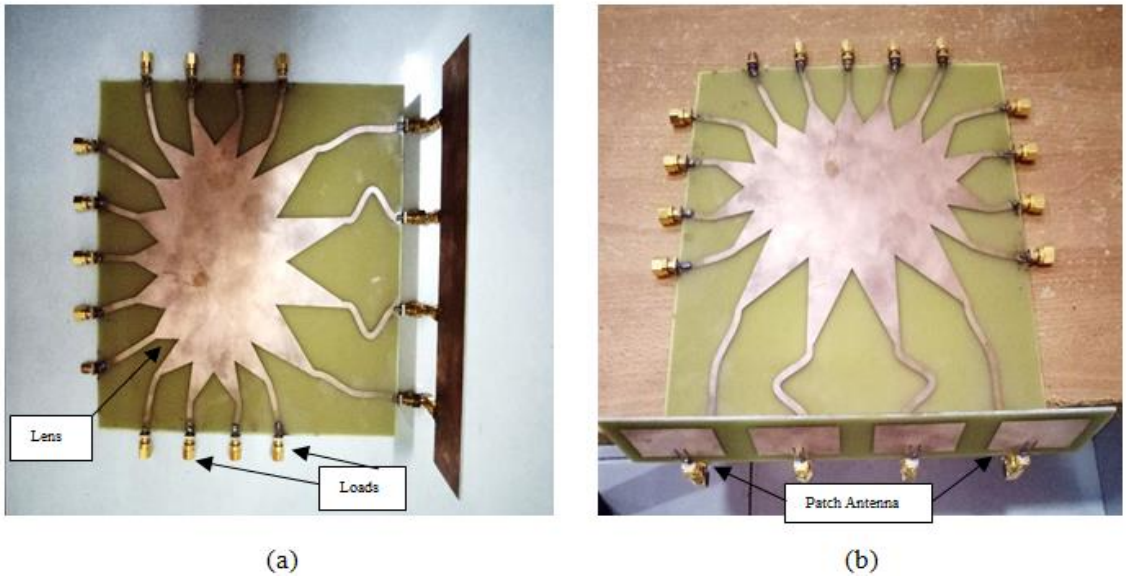

Figure 11. Full system beamforming: (a) top view (b) front view

Each beam port is excited by 2.45 GHz and all the other ports are terminated with 50Ω loads during the measurements. The simulation and measurement result of the radiation pattern for the five scanning beams are shown in Figure 13. It can be noted that the desired coverage angle ±26º are achieved in the azimuth plane with five scanning steps.

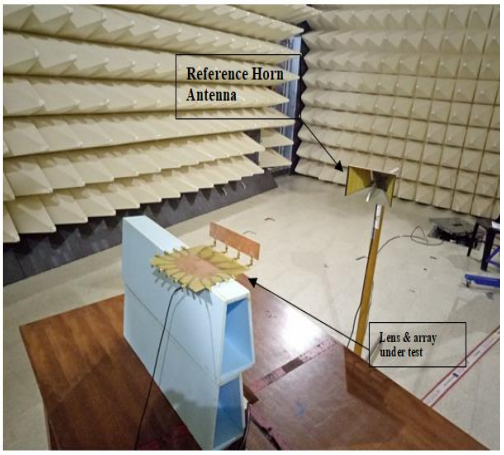

Figure 12. Measurements set up for radiation pattern

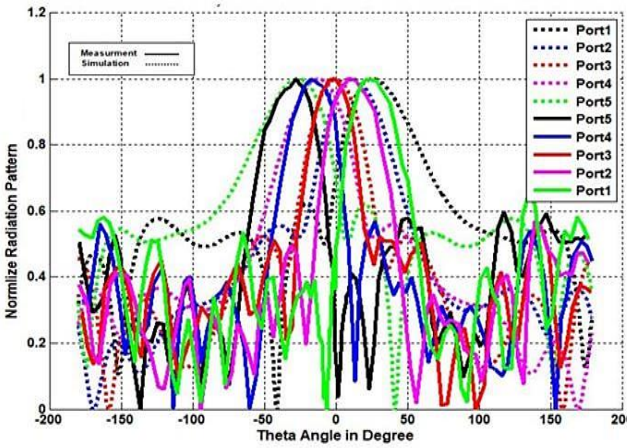

Figure 13. Radiation pattern for beamforming system at 2.45 GHz

4. Conclusion

A compact microstrip Rotman lens for wireless applications is proposed in this study to feed four element array and provide five scanning beams. A numerical parametric examination of the lens design structure to achieve low phase error for lens shape contour, relation between focal length and aperture size, and phase optimization factor β was applied. Eccentricity showed small effect to the phase error while minimum β provide maximum phase error for the selected lens specification. The proposed lens model is fabricated using FR-4 with a compact area of 209.52*203.62*1.6 mm^3. Five switching beams in azimuth plane are simulated and measured by excitation 2.45 GHz for each beam port. Five beams are generated to cover ±26º using four patch antenna. Besides, validation between simulation results using CST Microwave Studio and measurements is carried out for return loss, phase shifting, radiation pattern, and energy coupling between input ports and output ports. An agreement between numerical design procedures and measurements is achieved.

ACKNOWLEDGEMENTS

The authors would like to acknowledge ORICC Universiti Tun Hussein Onn Malaysia (UTHM) for supporting this work. This work was supported by research grants TIER 1 (vot no: U860).

References

[1] Mumcu G, Kacar M, Mendoza J. Mm-Wave Beam Steering Antenna With Reduced Hardware Complexity Using Lens Antenna Subarrays. *IEEE Antennas and Wireless Propagation Letters*. 2018; 17(9): 1603-1607.
[2] Aldrigo M. Smart two-dimensional material-based time modulated array for RFID applications. *IET Microwaves, Antennas and Propagation*. 2017; 11: 2267-2272.
[3] Singh A, Kumar A, Ranjan A, Kumar A, Kumar A. *Beam steering in antenna.* 2017 International Conference on Innovations in Information, Embedded and Communication Systems (ICIIECS). Coimbatore. 2017: 1-4.
[4] Pirapaharan K, Kunsei H, Senthilkumar KS, Hoole PRP, Hoole SRH. *A single beam smart antenna for wireless communication in a highly reflective and narrow environment*. 2016 International Symposium on Fundamentals of Electrical Engineering (ISFEE). Bucharest. 2016: 1-5.

[5] Gao S, Luo Q. *Low-cost smart antennas for advanced wireless systems*. 2014 International Workshop on Antenna Technology: Small Antennas, Novel EM Structures and Materials, and Applications (iWAT). Sydney. 2014: 132-135.
[6] Hansen RC. Phased Array Antennas. New York: John Wiley & Sons. 1998: 330-370.
[7] Mohsen MK, Isa Msm, Zakaria Z, Isa Aam, Abdulhameed MK, Attiah ML. Control Radiation Pattern for Half Width Microstrip Leaky Wave Antenna by Using PIN Diodes. *International Journal of Electrical and Computer Engineering (IJECE)*. 2018; 8(5): 2959-2966.
[8] Doucha S, Abri M, Badaoui HA, Fellah B. A Leaky Wave Antenna Design Based on Halfmode Substrate Integrated Waveguide Technology for X Band Applications. *International Journal of Electrical and Computer Engineering (IJECE)*. 2017; 7(6): 3467-3474.
[9] Esmail BAF, Majid HA, Abidin ZZ, Dahlan SH, Rahim MKA. Reconfigurable Metamaterial Structure at Millimeter Wave Frequency Range. *International Journal of Electrical and Computer Engineering (IJECE)*. 2017; 7(6): 2942-2949.
[10] Rotman W, Turner R. Wide-angle microwave lens for line source applications. *IEEE Transactions on Antennas and Propagation*. 1963 November; 11(6): 623–632.
[11] Metz C, Grubert J, Heyen J, Jacob AF, Janot S, Lissel E, et al. Fully integrated automotive radar sensor with versatile resolution. *IEEE Transactions on Microwave Theory and Techniques*. 2001; 49(12): 2560-2566.
[12] Holman B, Graham J, Skala J, Bing K, Bruna MA. *Using a Rotman lens as a substitute for a multi-channel antenna in a digitally beam-formed RADAR or SIGINT system*. 2015 IEEE Radar Conference (RadarCon). Arlington. 2015: 0490–0494.
[13] Zhang ZY, Zhao Y, Ji L, Zuo SL, Xu F, Fu G. Design of multi-beam antenna based on Rotman lens. *International Journal of RF and Microwave Computer-Aided Engineering*; 2018; 28(2): 1-10.
[14] Katagi T, Mano S, Sato S. An improved design method of Rotman lens antennas. *IEEE Transactions on Antennas and Propagation.* 1984; 32(5): 524-527.
[15] Smith MS. Design considerations for ruze and rotman lenses. *Radio and Electronic Engineer*. 1982; 52(4): 181-187.
[16] Rajabalian M. Optimisation and implementation for a non-focal Rotman lens design. *IET Microwaves, Antennas and Propagation.* 2015; 9: 982-987.
[17] Zaghloul AI, Dong J. A Concept for a Lens Configuration for 360_Scanning. *IEEE Antennas and Wireless Propagation Letters.* 2009; 8: 985-988.
[18] Uyguroğlu R, Öztoprak AY, Ergün C. Improved phase performance for rotman lens. *International Journal of RF and Microwave Computer-Aided Engineering*. 2012; 23(6): 634-638.
[19] Dong J, Zaghloul AI, Sun R, Reddy CJ, Weiss SJ. Rotman Lens Amplitude, Phase, and Pattern Evaluations by Measurements and Full Wave Simulations. *The Applied Computational Electromagnetics ACES Journal.* 2009; 24(6): 567-576.
[20] Penney CW, Luebbers RJ, Lenzing E. *Broad band Rotman lens simulations in FDTD*. 2005 IEEE Antennas and Propagation Society International Symposium. Washington. 2005; 2B: 51–54.
[21] Simon P. In: Analysis and Synthesis of Rotman Lenses.
[22] Dong J, Zaghloul AI. Hybrid Ray Tracing Method for Microwave Lens Simulation. *IEEE Transactions on Antennas and Propagation.* 2011; 59(10): 3786-3796.
[23] Balanis CA. Antenna theory: analysis and design. New York: John Wiley & Sons. 2005.
[24] Hansen RC. Design trades for Rotman lenses. *IEEE Transactions on Antennas and Propagation*. 1991; 39(4): 464-472.
[25] Al-Obaidi MK, Uyguroğlu R. *Microstrip Rotman lens fed array using multisection transition*. 2015 23nd Signal Processing and Communications Applications Conference (SIU). Malatya. 2015: 1106-1109.
[26] Junwei Dong, Zaghloul AI, Rensheng Sun, Reddy CJ. *EHF Rotman lens for electronic scanning antennas*. 2008 Asia-Pacific Microwave Conference. Macau. 2008: 1-4.
[27] Dong J, Zaghloul AI, Rotman R. Phase-error performance of multi-focal and non-focal two-dimensional Rotman lens designs. *IET Microwaves, Antennas Propagation*. 2010; 4(12): 2097-2103.
[28] Pozar DM. Microwave Engineering. Hoboken, NJ: John Wiley & Sons. 2012: 261-267.
[29] Dong J, Cheung R. *A computer synthesized 2-8 GHz printed Rotman Lens with 9*8 input-output configuration*. 2011 IEEE International Symposium on Antennas and Propagation (APSURSI). Spokane. 2011: 616-619